Adsorption of Arsenic and Lead onto Stone Powder and Chitosan-Coated Stone Powder

Authors:

Kyungho Jung, Sanghwa Oh, Hun Bak, Gun-Ho Song, Hong-Tae Kim

Date Submitted: 2019-11-24

Keywords: chitosan-coated stone powder, stone powder, Adsorption, lead, arsenic

Abstract:

Stone powder (SP) produced from masonry mills has been treated as a specific waste and rarely used for environmental purposes. In this study, we tested its potential as an adsorbent to remove arsenic (As) and lead (Pb) from water. The single-solute sorption isotherms for As(V) and Pb(II) onto SP and chitosan-coated SP (CSP) were investigated. Several sorption models, such as the Langmuir, Freundlich, and Dubinin?Radushkevich (DR) models, were used to analyze the adsorption features. The results demonstrated that As and Pb were successfully adsorbed onto SP and CSP, indicating that SP and CSP had potential as adsorbents of As and Pb. The maximum adsorption capacities of SP and CSP for Pb were 22.8 and 54.5 times higher than those for As, respectively. Chitosan coating increased the adsorption potential in Pb adsorption by 5% but decreased it in As adsorption. The adsorption potential also depended on the pH and temperature. The adsorption amount of As increased with pH but that of Pb decreased as pH increased. In addition, the ln b in the Langmuir model increased with 1/T (K), indicating that the adsorption of As and Pb occurred exothermically and spontaneously.

Record Type: Published Article

Submitted To: LAPSE (Living Archive for Process Systems Engineering)

Citation (overall record, always the latest version):	LAPSE:2019.1188
Citation (this specific file, latest version):	LAPSE:2019.1188-1
Citation (this specific file, this version):	LAPSE:2019.1188-1v1

DOI of Published Version: https://doi.org/10.3390/pr7090599

processes

MDPI

Article

Adsorption of Arsenic and Lead onto Stone Powder and Chitosan-Coated Stone Powder

Kyungho Jung [1], Sanghwa Oh [1,*], Hun Bak [2], Gun-Ho Song [1] and Hong-Tae Kim [2]

[1] School of Architectural, Civil, Environmental, and Energy Engineering, Kyungpook National University, Daegu 41566, Korea; chilbo4518@hanmail.net (K.J.); sgh0799@hanmail.net (G.-H.S.)
[2] Department of Civil Engineering, Kyungpook National University, Daegu 41566, Korea; hee08160@naver.com (H.B.); htkim@knu.ac.kr (H.-T.K.)
* Correspondence: shoh@knu.ac.kr; Tel.: +82-53-950-5609

Received: 20 August 2019; Accepted: 2 September 2019; Published: 5 September 2019

Abstract: Stone powder (SP) produced from masonry mills has been treated as a specific waste and rarely used for environmental purposes. In this study, we tested its potential as an adsorbent to remove arsenic (As) and lead (Pb) from water. The single-solute sorption isotherms for As(V) and Pb(II) onto SP and chitosan-coated SP (CSP) were investigated. Several sorption models, such as the Langmuir, Freundlich, and Dubinin–Radushkevich (DR) models, were used to analyze the adsorption features. The results demonstrated that As and Pb were successfully adsorbed onto SP and CSP, indicating that SP and CSP had potential as adsorbents of As and Pb. The maximum adsorption capacities of SP and CSP for Pb were 22.8 and 54.5 times higher than those for As, respectively. Chitosan coating increased the adsorption potential in Pb adsorption by 5% but decreased it in As adsorption. The adsorption potential also depended on the pH and temperature. The adsorption amount of As increased with pH but that of Pb decreased as pH increased. In addition, the ln b in the Langmuir model increased with 1/T (K), indicating that the adsorption of As and Pb occurred exothermically and spontaneously.

Keywords: arsenic; lead; adsorption; stone powder; chitosan-coated stone powder

1. Introduction

Given their frequency, toxicity, and potential for human exposure, arsenic (As) and lead (Pb) are the most prioritized substances by the Agency for Toxic Substances and Disease Registry (ATSDR) in the USA. One of their main exposure pathways is groundwater, one of the most important water supplies in the world. Therefore, groundwater pollution with As and Pb has been a great threat to the use of drinking water in countries worldwide such as China, Bangladesh, the USA, Nepal, Vietnam, Mexico, Argentina, Spain, Japan, India, and Korea [1–3]. Many people who have used groundwater as drinking water have been dying or suffering from diseases. In particular, long-term use of As- or Pb-contaminated groundwater can cause various kinds of cancers [4]. Despite these problems, groundwater is still a major source of drinking water [5]. Therefore, various technologies to remove As and Pb from groundwater chiefly and effectively have been researched.

Stone powder (SP) is mainly made of granite in Korea and produced from masonry mills or in the process of producing crushed sand. SP generally consists of SiO_2 and Al_2O_3 and is similar to Class F fly ash [6,7]. When mixed with water, SP has high strength, and thus, it can be recycled as a geopolymer or an admixture of concrete [7]. However, SP has been classified as a specific waste in Korea, and its huge production has been causing great environmental concern because of the potential of surface water and groundwater contamination, the relative lack of reuse or recycling, and its illegal disposal. In addition, there has been very little research on the environmental use of SP. Al-Jabari et al. [8] successfully used

stone cutting solid waste to adsorb organic materials in dairy wastewater. In this study, small amounts of iron powder were produced during the processing of stones due to the wear of saws, and the iron powder could be separated using a magnet. This iron powder was expected to be a good adsorbent for arsenic and heavy metals.

Chitosan-based adsorbents are receiving great attention due to their eco-friendly adsorption properties. Chitosan is very effective in adsorbing metals due to its high amino and carboxyl functional group content [9], and coating the surface of SP with chitosan can enhance SP's adsorption ability. Therefore, many researchers have attempted to coat the surface of adsorbents with chitosan to provide high adsorption capacities [9–11]. Qi and Xu [10] investigated the applicability of chitosan nanoparticles to lead sorption and found they could sorb Pb ions effectively with 398 mg/g of the maximum sorption capacity of Pb. Gupta et al. [11] presented that chitosan-coated sand (CCS) had a high arsenic adsorption capacity (23 mg/g) and was successfully applied for the removal of total inorganic arsenic (<10 μg/L) from arsenic-contaminated groundwater. In addition, we expected that chitosan could be used as a stone and iron powder linker due to its high adhesion feature [12]. Although chitosan is considered a good adsorbent and cross-linker, the use of chitosan alone would be expensive [11]. Coating the surface of inexpensive waste materials, such as SP with chitosan, would be one of the best ways to reduce the cost.

In this study, chitosan-coated stone powder (CSP) and stone powder (SP) were prepared, and their adsorption features were evaluated for the removal of As and Pb at various pH values. Several adsorption models (the Freundlich, Langmuir, and Dubinin–Radushkevich (DR) models) were used to fit the experimental data to explain the adsorption features. In addition, the temperature effect on adsorption was also investigated.

2. Materials and Methods

2.1. Materials

SP, granite sludge consisting mainly of SiO_2 and Al_2O_3, was obtained from a masonry mill in Yeongcheon, Korea. The collected SP samples were air-dried for more than 5 days and sieved through a 75 μm mesh (sieve #200), mixed, and stored in an airtight plastic container before use. Sodium arsenate dibasic heptahydrate (Na_2HAsO_4, >99.0%) was purchased from Wako, Japan. Lead nitrate ($Pb(NO_3)_2$, >99.0%) was purchased from Duksan Co., Korea. Chitosan produced from crab shell was purchased from Daejung Co., Korea. Acetic acid (CH_3COOH, >98.0%) used for dissolving chitosan was also purchased from Duksan Co., Korea. Hydrochloric acid (HCl, 35%–37%) was purchased from Duksan Co., Korea. MES (2-(*N*-morpholino)ethanesulfonic acid, >98.0%) and sodium bicarbonate (NaHCO, >99.0%), used as a pH buffer, were also purchased from Daejung Co., Korea.

2.2. Preparation of CSP

In order to enhance the field application of SP, it was coated with the chitosan through modification of Gupta's method [12]. Briefly, SP was washed twice with deionized (DI) water (Milli-Q, 18 MΩ-cm) and 1 M HCl to remove the adsorbed metal ions and dried at 90 °C for 20 h to activate the salts.

For the chitosan coating process, chitosan was dissolved in 0.05 M acetic acid to make the final concentration of 0.5% by weight. The activated SP was mixed with the chitosan solution. The mixture was stirred overnight, washed with DI water, and then dried at room temperature before use.

2.3. Physicochemical Analysis of SP and CSP

The specific surface areas of SP and CSP were measured from N_2 adsorption isotherms by the Brunauer–Emmett–Teller (BET) method (BET Quantachrome, Autosorb-iQ, Florida, FL, USA). The X-ray diffraction (XRD) of SP and CSP was carried out using an X-ray diffractometer (D/Max-2500, Rigaku, Japan). A field emission scanning electron microscope (FE-SEM, SU8220, Hitachi, Japan) was applied to observe the morphology of the adsorbents, and an energy dispersive X-ray spectroscope

(EDS, Horiba E-MAX EDS detector, Japan) was also used to characterize the chemical compositions. The BET, FE-SEM, and EDS analyses were conducted at the Instrumental Analysis Center of Kyungpook National University, Korea. The X-ray fluorescence (XRF) analyses were conducted using a wavelength dispersive X-ray fluorescence spectrometer (WD-XRF) at the Korea Basic Science Institute (Daegu). The point of zero charge (PZC) was determined by a batch method [13].

2.4. Adsorption Experiment

Adsorption isotherms for As and Pb were determined in SP and CSP to ascertain the effect of chitosan coating on As and Pb adsorption features. The standard batch technique was used in this study. Briefly, As and Pb solutions with 0.001 to 1.21 mmol/L and 200 to 2000 mg/L, respectively, were prepared. Approximately 1 g, on a dry weight basis, of SP or CSP was added to 50 mL of artificially As- or Pb-contaminated water in screw-cap conical tubes. The tubes were capped tightly, shaken at 200 rpm for 24 h in an orbital shaker. Preliminary equilibrium time experiments showed less than 6 h for both As and Pb adsorptions (data not shown). After mixing, the tubes were collected and centrifuged at 2000 rpm for 10 min. The supernatant was filtrated through a 0.2 μm membrane filter (cellulose nitrate membrane, Whatman). The As and Pb concentrations in the aqueous phases were analyzed using a inductively coupled plasma (ICP, Optima 2100 DV, PerkinElmer, Sweden).

An experiment on the effect of pH on the adsorption of As and Pb was also conducted by adjusting the pH of the metal solutions to 4, 7, and 9 for As adsorption, and 3, 4.5, and 7 for Pb adsorption using MES and bicarbonate buffers. The pH buffers used in this study did not affect As and Pb adsorption [14,15]. The adsorption step for the pH effect experiment was the same as that for the adsorption isotherm experiment. To investigate the effect of temperature on adsorption, the adsorption isotherm experiments were conducted at three different temperatures (20 °C, 30 °C, and 40 °C). All experiments were conducted in duplicate.

The adsorbed amount, q (mmol/kg), was calculated using Equation (1):

$$q = \frac{(C_0 - C)V}{W}, \tag{1}$$

where C_0 is the initial solute concentration (mmol/L), C is the residual solute concentration (mmol/L), V is the sample volume (L), and W is the weight of the adsorbent, such as SP or CSP ($\times 10^{-3}$ kg).

2.5. Isotherm Model

The adsorbed amount (q) against the equilibrium concentration of solute in solution (C) was plotted and evaluated with several adsorption isotherm models such as the Freundlich, Langmuir, and DR models.

The Freundlich model was developed to describe monolayer gas adsorption on heterogeneous solids, and it provides a basic equation for understanding nonlinear adsorption [16]. The Freundlich equation can be expressed as:

$$q = K_F C^N, \tag{2}$$

where K_F is the adsorption capacity, and the exponent [(mmol/kg)/(mmol/L)^N], N, characterizes the energy distribution of the adsorption sites (unitless). $N < 1$ indicates nonlinear adsorption, where the marginal adsorption energy decreases with increasing surface concentration [16].

The Langmuir model was formulated for monolayer adsorption on homogeneous surfaces. The equation can be expressed as:

$$q = \frac{q_{mL} b C}{1 + bC}, \tag{3}$$

where q_{mL} is the maximum adsorption capacity (mmol/kg), and b is characterized as constant adsorption energy (L/mmol).

The DR model is generally applied to express the adsorption mechanism with a Gaussian energy distribution on heterogeneous surfaces [17,18], and therefore, it can distinguish between physical and chemical adsorption characteristics [19]:

$$q = q_{mD} \exp(-\beta\varepsilon^2) = q_{mD} \exp\left[-\beta\left(RT \ln\left(1 + \frac{1}{C}\right)\right)^2\right], \quad (4)$$

where q_{mD} is the theoretical saturation capacity (mmol/kg), β is characterized as the mean free energy of adsorption per mole of sorbate (mol^2/J^2), and ε is the Polanyi potential:

$$\varepsilon = RT \ln\left(1 + \frac{1}{C}\right), \quad (5)$$

where R is the gas constant (8.314 J/mol·K), and T (K) is the absolute temperature. The mean free energy E (J/mol) can be calculated from β:

$$E = \frac{1}{\sqrt{2\beta}}. \quad (6)$$

2.6. Thermodynamic Analysis

Thermodynamic analyses of the adsorption were conducted to estimate whether the reaction was spontaneous or not. The Langmuir parameter, b, was used as the thermodynamic parameter for Gibb's free energy change, $\Delta G°$ (kJ/mol), in the adsorption process. The change in Gibb's free energy is a negative value if the reaction occurs spontaneously. The changes in enthalpy, $\Delta H°$ (kJ/mol), and entropy, $\Delta S°$ (J/mol/K), are calculated using [20,21]:

$$\Delta G^0 = -RT \ln b \quad (7)$$

$$\Delta G^0 = \Delta H^0 - T\Delta S^0. \quad (8)$$

These equations can be expressed as:

$$\ln b = \frac{\Delta S^0}{R} - \frac{\Delta H^0}{RT}. \quad (9)$$

As shown in Equation (9), a plot of ln b vs. $1/T$ can give other thermodynamic parameters, such as the change of enthalpy and entropy [21].

3. Results

3.1. SP and CSP Characteristics

The specific area, pore volume, pore size, and pH values of SP and CSP are summarized in Table 1. The surface areas of SP and CSP were 2.78 and 2.64 m^2/g, respectively. The pore volume and pore size were 0.017 cm^3/g and 24.83 nm for SP, and 0.015 cm^3/g and 22.77 nm for CSP, respectively, indicating that SP has a relatively larger pore volume and pore size due to the thin chitosan-coated layer. The results of the XRD analyses of SP and CSP are shown in Figure 1. The XRD patterns of SP and CSP showed that SP contained a series of quartz (SiO_2) with the main peak at 2θ = 26.6° [22]. The results of the XRF analyses for SP and CSP are summarized in Table 2. The XRF results also revealed that SiO_2 was the main component of SP and CSP (65.69% and 66.11%, respectively); Al_2O_3, CaO, and Fe_2O_3 were also mainly detected.

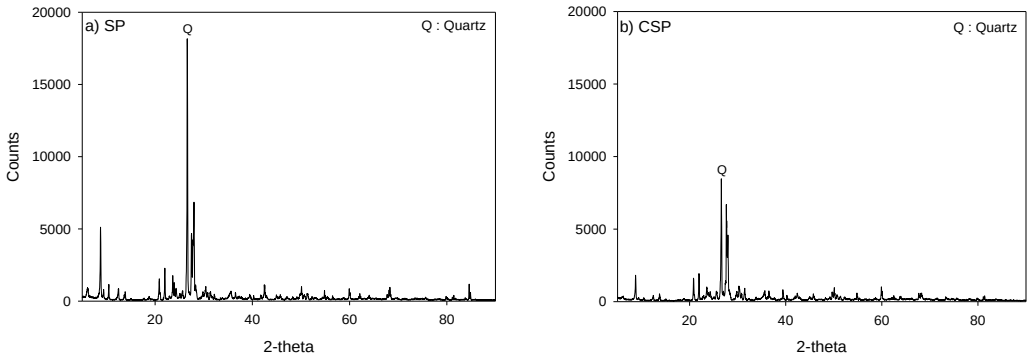

Figure 1. Results of XRD analyses of (**a**) stone powder (SP) and (**b**) chitosan-coated SP (CSP).

Table 1. Surface area, pore volume, pore size, and pH of SP and CSP.

	SP	CSP
BET surface area (m^2/g)	2.78	2.64
Pore volume (cm^3/g)	0.017	0.015
Pore size (nm)	24.83	22.77
pH	4.7	4.9

Table 2. Results of the X-ray fluorescence (XRF) analyses for SP and CSP.

Component	SP	CSP
Al_2O_3	16.22	16.19
CaO	4.57	4.60
Fe_2O_3	4.03	3.49
K_2O	2.69	2.61
MgO	2.50	2.34
Na_2O	2.94	2.98
SiO_2	65.69	66.11
L.O.I.	0.74	1.11

Figure 2 shows the surface morphologies (SEM images) and the EDS X-ray microanalyses of SP (a) and CSP (b). The SEM images show that the difference in the surface morphologies of SP and CSP was not significant. The EDS analyses were conducted on several particles, and the results showed that Si, Mg, O, Al, and Fe were prominent elements for both SP and CSP.

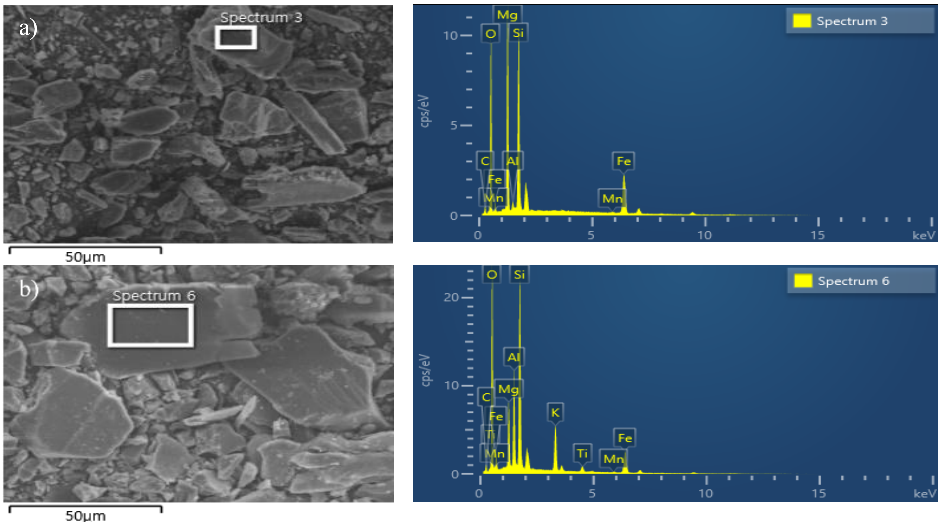

Figure 2. SEM images and EDS analyses for (**a**) SP and (**b**) CSP.

Figure 3 elucidates a point of zero salt effect (PZSE) as the PZC in SP and CSP. The PZSE is the pH value at the crossover point of potentiometric titration curves obtained at different ionic strengths [13,23]. The results showed that the PZSE of SP (8.25) was higher than that of CSP (4.5), perhaps because the SP surface was coated with chitosan dissolved in acetic acid.

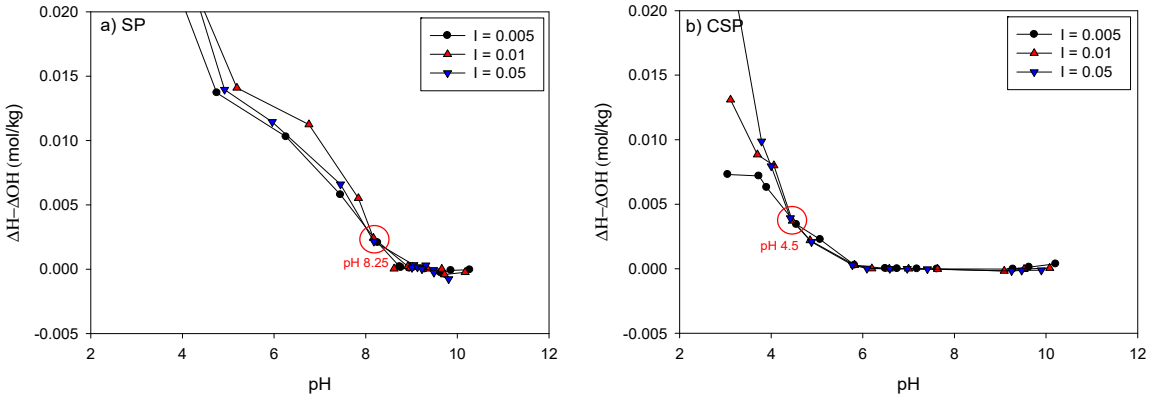

Figure 3. The point of zero charge (PZC) for (**a**) SP and (**b**) CSP.

3.2. As and Pb Adsorption onto SP and CSP

The solution speciations of As and Pb were calculated using Visual MINTEQ (Version 3.1, Sweden), and they are shown in Figure 4. $H_2AsO_4^-$ was the dominant As species at a pH between 3 and 6, and the dominant Pb^{2+} species at a pH below 7. $PbOH^+$ and $Pb_3(OH)_4^{+2}$ were dominant at a pH of 7 to 8 and 8 to 10, respectively. Therefore, $H_2AsO_4^-$ and Pb^{2+} ions were dominant in solution at pH 4 to 4.5, $HAsO_4^{-2}$ and $Pb^{2+}/PbOH^+$ were dominant at pH 7, and $HAsO_4^{-2}$ and $Pb_3(OH_4)^{+2}$ were dominant at pH 9, as shown in Figure 4. At a pH above 11, $Pb(OH)_3^-$ was dominant.

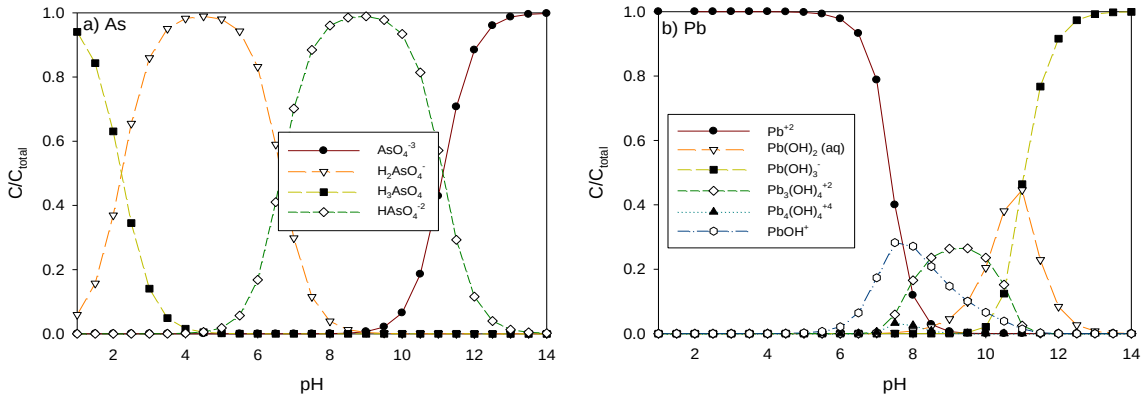

Figure 4. Distribution of (**a**) As and (**b**) Pb compounds as a function of pH predicted by Visual MINTEQ 3.1 software.

Figure 5 shows the adsorption isotherm patterns of As and Pb onto SP and CSP at three different pH conditions: 4, 7, and 9 for As adsorption, and 3, 4.5, and 7 for Pb adsorption. The isotherm model parameters for the Freundlich, Langmuir, and DR models are summarized in Table 3 (for As) and Table 4 (for Pb). All adsorption patterns showed nonlinear L-type adsorption, indicating that strong interactions between adsorbate (As or Pb) and adsorbent (SP or CSP) occurred [15]. As shown in Table 3, all models had a similar range of the coefficient of determination (R^2) for each of the pH values. The R^2 values were in the range of 0.762 to 0.900 for SP, and 0.611 to 0.942 for CSP for all models. Table 4 shows that the R^2 values of the isotherm models for SP (0.678 to 0.928) were higher than those for CSP (0.569 to 0.816). The Freundlich and Langmuir models showed a better fit than the DR model.

For estimating the effect of chitosan coating on As and Pb adsorption, the adsorption results of As and Pb were compared at the same pH. A comparison of Tables 3 and 4 shows that Pb is more attracted for adsorption onto SP and CSP than As. The amount of As adsorbed on SP was higher than that on CSP at the same pHs, whereas the amount of Pb adsorbed on CSP was higher than that on SP, as shown in Figure 5.

For example, at pH 4, the maximum amount (q_{mL}) of As adsorbed onto SP (1.838 mmol/kg) was higher than that onto CSP (0.957 mmol/kg), whereas the maximum amount of Pb adsorbed onto SP (41.88 mmol/kg) was less than that onto CSP (52.18 mmol/kg) at pH 4.5. This indicates that the chitosan coating decreased the sorption capability of SP for As but increased it for Pb. The chitosan was known as a good adsorbent for As, but in this study, the chitosan coating had a negative effect on adsorption affinity of As. Anto and Annadurai [24] also studied the effect of concentration of the chitosan nanoparticle from 0.5% to 1.2% on As adsorption capacity onto chitosan nanoparticle immobilized into sodium alginate and found the decreasing pattern of As adsorption capacity from 21.7 mg/g at 0.5% to 16.7 mg/g at 1.2%, except 23.7 mg/g at 1.0%. In this study, although the pH was adjusted by pH buffer solutions, the final pH value increased to the range of 4.5 to 5.6 during adsorption. The final pH was higher than the PZC value of CSP (4.5), which indicates a negative charge of the CSP surface. In addition, As compounds also exist with a negative charge as pH increases, which produces the repulsion forces between As compounds and SP or CSP [12]. On the other hand, because Pb is positively charged, it is easily adsorbed to negatively charged SP and CSP particles [25,26]. The maximum adsorption amount of Pb at a pH of 4.5 was about 20 to 50 times higher than that of As at pH 4, according to q_{mL} and q_{mD}. K_F values in the Freundlich model for As adsorption were lower than those for Pb adsorption due to the higher adsorption affinity of Pb. The N values in the Freundlich model were in the range of 0.248 to 0.738 for As and 0.221 to 0.431 for Pb, indicating that As and Pb adsorption was nonlinear and favorable [27].

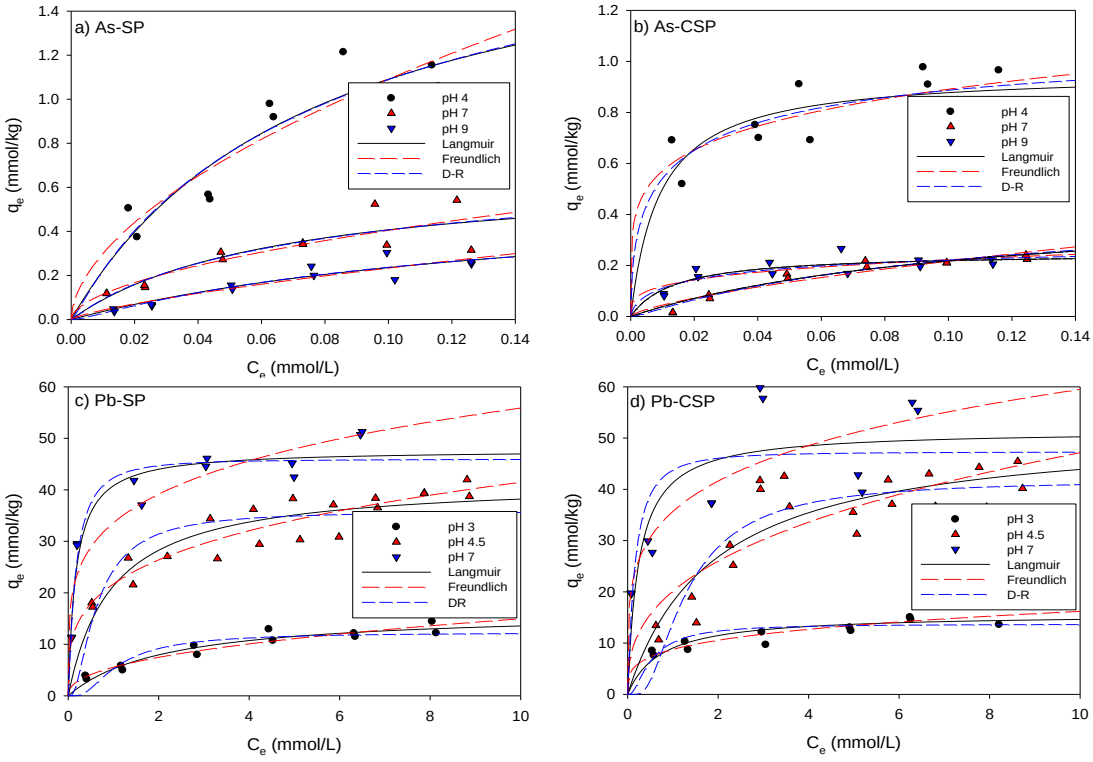

Figure 5. Effect of pH on (**a**,**b**) As and (**c**,**d**) Pb adsorption onto (**a**,**c**) SP and (**b**,**d**) CSP.

Table 3. Isotherm model parameters for As adsorption onto SP and CSP at pH 4, 7, and 9.

Model	Parameter	SP			CSP		
		pH 4	**pH 7**	**pH 9**	**pH 4**	**pH 7**	**pH 9**
Freundlich	K_F (mmol^{1-N} L^N/kg)	4.072	1.432	1.277	1.602	1.051	0.416
	N (-)	0.572	0.549	0.738	0.248	0.686	0.273
	R^2	0.899	0.762	0.860	0.790	0.899	0.611
Langmuir	q_{mL} (mmol/kg)	1.838	0.672	0.605	0.957	0.455	0.249
	b (L/mmol)	14.45	15.41	6.385	109.3	9.214	71.84
	R^2	0.900	0.776	0.878	0.811	0.934	0.705
DR	q_{mD} (mmol/kg)	1.883	0.706	0.521	1.111	0.450	0.287
	β (mol^2/kJ^2), $\times 10^{-2}$	1.569	1.563	2.229	0.610	2.031	0.728
	E (kJ/mol)	5.646	5.656	4.736	9.056	4.962	8.287
	R^2	0.900	0.774	0.883	0.815	0.942	0.661

Table 4. Isotherm model parameters for Pb adsorption onto SP and CSP at pH 3, 4.5, and 7.

Model	Parameter	SP			CSP		
		pH 3	**pH 4.5**	**pH 7**	**pH 3**	**pH 4.5**	**pH 7**
Freundlich	K_F (mmol^{1-N} L^N/kg)	5.540	21.73	33.59	8.777	20.11	35.67
	N (-)	0.431	0.281	0.221	0.266	0.370	0.222
	R^2	0.922	0.856	0.872	0.816	0.703	0.731
Langmuir	q_{mL} (mmol/kg)	16.47	41.88	47.77	15.69	52.18	51.49
	b (L/mmol)	0.466	1.037	5.833	1.358	0.529	4.040
	R^2	0.923	0.805	0.928	0.700	0.779	0.659
DR	q_{mD} (mmol/kg)	12.27	35.86	45.96	13.69	41.76	47.31
	β (mol^2/kJ^2), $\times 10^{-2}$	28.85	13.10	2.802	10.36	37.18	2.666
	E (kJ/mol)	1.317	1.953	4.224	2.197	1.160	4.330
	R^2	0.788	0.678	0.926	0.569	0.783	0.601

The isotherm parameters affected by pH can be identified in Tables 3 and 4. K_F in the Freundlich model, q_{mL} in the Langmuir model, and q_{mD} in the DR model were affected by pH. K_F, q_{mL}, and q_{mD} decreased in the case of As adsorption as pH increased but increased in the case of Pb adsorption. This indicates that the adsorption affinity, K_F, and the maximum capacity (q_{mL} and q_{mD}) of SP and CSP decreased with pH in the case of As adsorption but increased with pH in the case of Pb adsorption. However, N in the Freundlich model, b in the Langmuir model, and β and E in the DR model varied irregularly regardless of pH.

Figure 6a shows the linear relationship (R^2 = 0.990) between q_{mL} in the Langmuir model and q_{mD} in the DR model for As and Pb adsorption. This means that the maximum amounts of As and Pb adsorption were very similar even though the adsorption mechanisms of the Langmuir and DR models differed. Theoretically, b in the Langmuir model is known to be related to the adsorption energy [28,29]. The relationship between ln b in the Langmuir model and E calculated from the DR model was plotted in Figure 6b, and b turned out to be very close to E with high R^2 (0.9897).

From the result of Figure 6b, Equations (7)–(9) were used to determine Gibb's free energy with ln b for As and Pb adsorptions onto SP and CSP at several temperatures (293, 303, and 313 K). Plotting 1/T and ln b for As and Pb onto SP and CSP shows good linear regression with a positive slope (Figure 7). The values of ΔG°, ΔH°, and ΔS° are summarized in Table 5. The negative values of ΔG° indicate that the As and Pb adsorption process was spontaneous and favorable with increasing temperature [30]. The negative values of ΔH° show that the adsorption process was exothermic for As and Pb adsorption onto SP and CSP. However, the ΔS° value was positive for As adsorption onto SP and CSP, which denotes increased randomness during adsorption but negative randomness for Pb adsorption, which indicates decreased randomness.

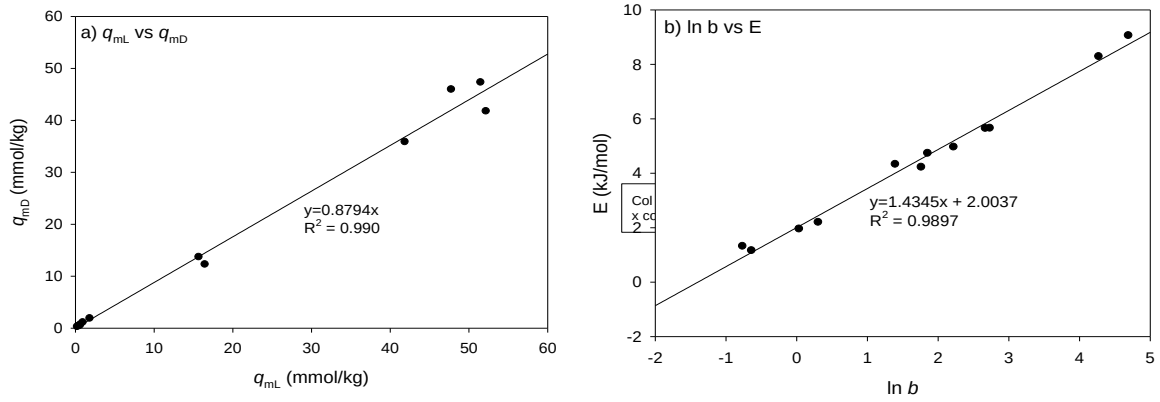

Figure 6. Relationship between (**a**) q_{mL} and q_{mD}, and (**b**) ln *b* and *E*.

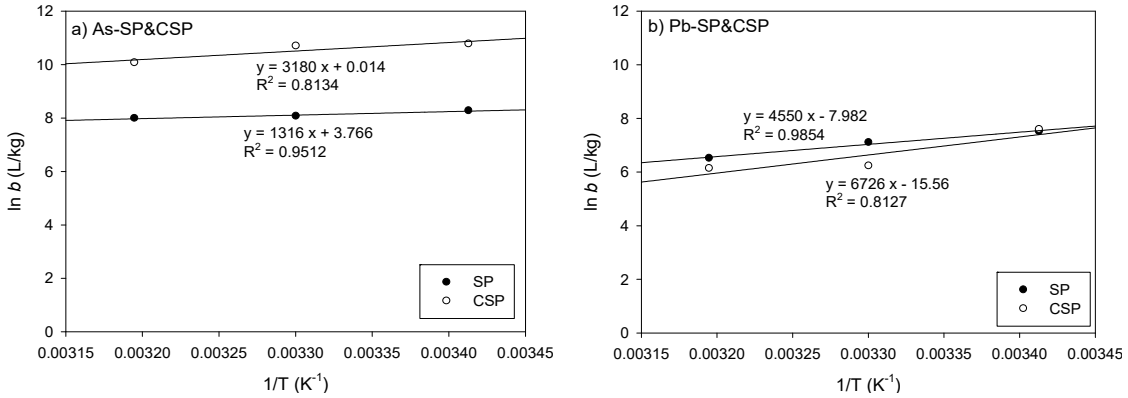

Figure 7. Relationship between 1/T and ln *b* for (**a**) As and (**b**) Pb.

Table 5. Results of thermodynamic analyses for As and Pb adsorption at 293, 303, and 313 K.

Material	Parameter	SP			CSP		
		293° K	**303° K**	**313° K**	**293° K**	**303° K**	**313° K**
As	ln *b*	8.276	8.073	7.991	10.78	10.70	10.08
	b-based ΔG° (kJ/mol)	−20.16	−20.34	−20.79	−26.25	−26.96	−26.22
	b-based ΔS° (kJ/mol/K)		0.0313			0.00012	
	b-based ΔH° (kJ/mol)		−10.94			−26.44	
Pb	ln *b*	7.513	7.104	6.518	7.592	6.232	6.139
	b-based ΔG° (kJ/mol)	−18.30	−17.90	−16.96	−18.50	−15.70	−15.98
	b-based ΔS° (kJ/mol/K)		−0.0664			−0.1294	
	b-based ΔH° (kJ/mol)		−37.83			−55.92	

4. Conclusions

The adsorptive removal of As and Pb was successfully conducted using SP and CSP in this study. As and Pb could be adsorbed onto both SP and CSP, but Pb adsorption was more favorable for both adsorbents. The maximum amount of Pb adsorption was higher than that of As because chitosan has some functional groups (amine and hydroxyl groups) that are favorable to metal adsorption. The pH was also a major factor affecting the adsorption of As and Pb. The adsorbed amount of As decreased as the pH increased, whereas that of Pb increased. Therefore, the pH should be adjusted according to the target material of concern. The results of thermodynamic analyses indicated that the adsorption of As and Pb onto SP and CSP with negative ΔG° values was spontaneous.

Author Contributions: Conceptualization, S.O. and K.J.; methodology, S.O., K.J., G.-H.S., and H.B.; software, S.O.; formal analysis, S.O. and H.-T.K.; data curation, S.O. and H.B.; writing—original draft preparation, S.O.; writing—review and editing, S.O. and H.-T.K.

Funding: This research was supported by the Kyungpook National University Fund, 2017.

Acknowledgments: The authors are grateful to Kyungpook National University for supporting this research.

Conflicts of Interest: The authors declare no conflict of interest.

References

1. Jain, C.K.; Singh, R.D. Technological options for the removal of arsenic with special reference to South East Asia. *J. Environ. Manag.* **2012**, *107*, 1–18. [CrossRef] [PubMed]
2. Jiang, J.Q.; Ashekuzzaman, S.M.; Jiang, A.; Shrifuzzaman, S.M.; Chowdhury, S.R. Arsenic contaminated groundwater and its treatment options in Bangladesh. *Int. J. Environ. Res. Public Health* **2013**, *10*, 18–46. [CrossRef] [PubMed]
3. Clausen, J.L.; Bostick, B.; Korte, N. Migration of lead in surface water, pore water, and groundwater with a focus on firing ranges. *Crit. Rev. Environ. Sci. Technol.* **2011**, *41*, 1397–1448. [CrossRef]
4. Zhu, J.; Lou, Z.; Liu, Y.; Fu, R.; Baig, S.A.; Xu, X. Adsorption behavior and removal mechanism of arsenic on graphene modified by iron-manganese binary oxide (FeMnOx/RGO) from aqueous solutions. *RSC Adv.* **2015**, *5*, 67951–67961. [CrossRef]
5. Phan, K.; Sthiannopkao, S.; Kim, K.Y.; Wong, M.H.; Sao, V.; Hashim, J.H.; Yasin, M.S.M.; Aljunid, S.M. Health risk assessment of inorganic arsenic intake of Cambodia residents through groundwater drinking pathway. *Water Res.* **2010**, *44*, 5777–5788. [CrossRef] [PubMed]
6. Choi, S.J.; Jun, S.S.; Oh, J.E.; Monteiro, P.J.M. Properties of alkali-activated systems with stone powder sludge. *J. Mater. Cycles Waste Manag.* **2010**, *12*, 275–282. [CrossRef]
7. Kim, J.M.; Jeong, J.Y.; Choi, S.J.; Kim, B.J. The density and strength properties of light weight foamed concrete using stone-powder sludge in hydrothermal reaction condition. *J. Korea Concr. Inst.* **2006**, *18*, 687–693.
8. Al-Jabari, M. Kinetics mass transfer adsorption model for treating dairy wastewater with stone cutting solid waste. *Environ. Technol. Innov.* **2017**, *7*, 21–29. [CrossRef]
9. Hasan, S.; Krishnaiah, A.; Ghosh, T.K.; Viswanath, D.S.; Boddu, V.M.; Smith, E.D. Adsorption of chromium(VI) on chitosan-coated perlite. *Sep. Sci. Technol.* **2003**, *38*, 3775–3793. [CrossRef]
10. Qi, L.; Xu, Z. Lead sorption from aqueous solutions on chitosan nanoparticles. *Colloids Surf. A Physicochem. Eng. Asp.* **2004**, *251*, 183–190. [CrossRef]
11. Gupta, A.; Yunus, M.; Sankararamakrishnan, N. Chitosan- and iron-chitosan-coated sand filters: A cost-effective approach for enhanced arsenic removal. *Ind. Eng. Chem. Res.* **2013**, *52*, 2066–2072. [CrossRef]
12. Cho, D.W.; Jeon, B.H.; Chon, C.M.; Schwartz, F.W.; Jeong, Y.; Song, H. Magnetic chitosan composite for adsorption of cationic and anionic dyes in aqueous solution. *J. Ind. Eng. Chem.* **2015**, *28*, 60–66. [CrossRef]
13. Sparks, D.L.; Page, A.I.; Helmke, P.A.; Loeppert, R.H.; Soltanpour, P.N.; Tabatabai, M.A.; Johnston, C.T.; Sumner, M.E. *Methods of Soil Analysis Part 3 Chemical Methods*, 1st ed.; Soil Science Society of America, Inc.; American Society of Agronomy, Inc.: Madison, WI, USA, 1996; pp. 1244–1248.
14. Niazi, N.K.; Burton, E.D. Arsenic sorption to nanoparticulate mackinawite (FeS): An examination of phosphate competition. *Environ. Pollut.* **2016**, *218*, 111–117. [CrossRef] [PubMed]
15. Oh, S.; Kwak, M.Y.; Shin, W.S. Competitive sorption of lead and cadmium onto sediments. *Chem. Eng. J.* **2009**, *152*, 376–388. [CrossRef]
16. Farrell, J.; Relnhard, M. Descorption of halogenated organics from model solids, sediments, and soil under unsaturated conditions. 1. Isotherms. *Environ. Sci. Technol.* **1994**, *28*, 53–62. [CrossRef] [PubMed]
17. Dada, A.O.; Olalekan, A.P.; Olatunya, A.M.; DaDa, O. Langmuir, Freundlich, Temkin and Dubinin-Radushkevich isotherms studies of equilibrium sorption of Zn^{2+} onto phosphoric acid modified rice husk. *IOSR J. Appl. Chem.* **2012**, *3*, 38–45.
18. Horsfall, M.; Spiff, A.I.; Abia, A.A. Studies on the influence of mercaptoacetic acid (MAA) modification of cassava (manihot sculenta cranz) waste biomass on the adsorption of Cu^{2+} and Cd^{2+} from aqueous solution. *Korean Chem. Soc.* **2004**, *25*, 969–976.
19. Kundu, S.; Gupta, A.K. Arsenic adsorption onto iron oxide-coated cement (IOCC): Regression analysis of equilibrium data with several isotherm models and their optimization. *Chem. Eng. J.* **2006**, *122*, 93–106. [CrossRef]

20. Liu, Y. Is the free energy change of adsorption correctly calculated? *J. Chem. Eng. Data* **2009**, *54*, 1981–1985. [CrossRef]
21. He, J.; Hong, S.; Zhang, L.; Gan, F.; Ho, Y.S. Equilibrium and thermodynamic parameters of adsorption of methylene blue onto rectorite. *Fresenius Environ. Bull.* **2010**, *19*, 2651–2656.
22. Chisholm, J. Comparison of quartz standards for X-ray diffraction analysis: HSE A9950 (Skiron F600) and NIST SRM 1878. *Ann. Occup. Hyg.* **2005**, *49*, 351–358. [PubMed]
23. Appel, C.; Ma, L.Q.; Rhue, R.D.; Kennelley, E. Point of zero charge determination in soils and minerals via traditional methods and detection of electroacoustic mobility. *Geoderma* **2003**, *113*, 77–93. [CrossRef]
24. Anto, S.M.; Annadurai, G. Arsenic adsorption from aqueous solution using chitosan nanoparticle. *Res. J. Nanosci. Nanotechnol.* **2012**, *2*, 31–45.
25. Hamed, I.; Ozogul, F.; Regenstein, J.M. Industrial application of crustacean by-products (chitin, chitosan, and chitoloigosaccharides): A review. *Trends Food Sci. Technol.* **2016**, *48*, 40–50. [CrossRef]
26. Zhang, L.; Zeng, Y.; Cheng, Z. Removal of heavy metal ions using chitosan and modified chitosan: A review. *J. Mol. Liquids.* **2016**, *214*, 175–191. [CrossRef]
27. Suteu, D.; Bilba, D.; Dan, F. Synthesis and characterization of polyamide powders for sorption of reactive dyes from aqueous solutions. *J. Appl. Polym. Sci.* **2007**, *105*, 1833–1843. [CrossRef]
28. Kamau, J.; Kamau, G. Modeling of experimental adsorption isotherm data for chlorothalonil by Nairobi river sediment. *Mod. Chem. Appl.* **2017**, *5*, 1–7.
29. Ayawei, N.; Ebelegi, A.N.; Wankasi, D. Modelling and interpretation of adsorption isotherms. *J. Chem.* **2017**, *2017*, 3039817. [CrossRef]
30. Khelaifia, F.Z.; Hazourli, S.; Nouacer, S.; Rahima, H. Valorization of raw biomaterial waste-date stones-for Cr (VI) adsorption in aqueous solution: Thermodynamics, kinetics and regeneration studies. *Int. Biodeterior. Biodegrad.* **2016**, *114*, 76–86. [CrossRef]